Role of Disulfide Linkages in Tachyplesin–Lipid Interactions

Katsumi Matsuzaki,* Mitsuya Nakayama, Masaru Fukui, Akira Otaka, Susumu Funakoshi, Nobutaka Fujii, Kiyoshi Bessho, and Koichiro Miyajima

Faculty of Pharmaceutical Sciences, Kyoto University, Sakyo-ku, Kyoto, 606-01 Japan

Received March 10, 1993; Revised Manuscript Received July 9, 1993®

ABSTRACT: In order to elucidate the role of the two disulfide linkages of tachyplesin I (T-SS), a membrane-acting cyclic antimicrobial peptide from *Tachypleus tridentatus*, we synthesized the acyclic analog (T-Acm) with the four SH groups protected by acetamidomethyl groups and also investigated the interactions of these peptides with lipid bilayers. T-SS induced leakage of calcein from egg yolk L-α-phosphatidylglycerol large unilamellar vesicles (PG LUVs) at peptide concentrations 1 order of magnitude smaller than those at which leakage was induced by T-Acm, which coincides with the stronger antimicrobial activities of T-SS. The micellization of PG LUVs was also more efficient for the cyclic peptide. Fluorescence titration studies revealed that binding affinities of both peptides to the PG membranes were similar. Fourier transform infrared polarized attenuated total reflection spectroscopy and fluorescence quenching experiments demonstrated that T-SS and T-Acm both form amphiphilic antiparallel β-sheet structures in the membranes. They are formed in such a way that the sheet planes lie parallel to the membrane surface with the sheet hydrophobic surfaces penetrating slightly into the hydrophobic region of the bilayers. Furthermore, the observation that the linear T-Acm, the weaker membrane permeabilizer, caused a far more serious membrane disruption suggests the possibility that the mechanisms of membrane permeabilization by the cyclic peptide are different from those by the linear peptide, the latter being the disruption of the lipid organization.

Tachyplesin I (T-SS),[1] which was isolated from the acid extracts of hemocytes of a horseshoe crab (*Tachypleus tridentatus*), is a cyclic antimicrobial peptide consisting of 17 amino acid residues (Figure 1; Nakamura et al., 1988). The peptide inhibits the growth of not only ordinary Gram positive and negative bacteria but also methicillin-resistant *Staphylococcus aureus* and fungi (Ohta et al., 1992). Two-dimensional NMR studies (Kawano et al., 1990; Tamamura et al., 1993b) revealed that the peptide forms a rigid antiparallel β-sheet structure, because of the two S–S linkages. The action mechanisms are thought to be based on the permeabilization of bacterial cell membranes (Matsuzaki et al., 1991c; Ohta et al., 1992), although the interactions with lipopolysaccharides (Nakamura et al., 1988) and DNA (Yonezawa et al., 1992) may also contribute to its bactericidal action. The amphiphilicity of the peptide appears to be important to its binding to these bacterial components. We have reported (Matsuzaki et al., 1991c, 1993) that (1) tachyplesin I specifically permeabilizes acidic lipid bilayers, (2) its Trp^2 residue is located in a hydrophobic region near the bilayer surface, and (3) the peptide micellizes the acidic lipid bilayers at low lipid to peptide ratios (L/P) around 7, where the peptide charge (+7) neutralizes the membrane charge; however, the membrane permeabilization is not because of micellization.

While the molecular mechanisms of the peptide are elucidated, it would be useful to clarify the role of the disulfide bonds. Linear analogs of tachyplesin I have been reported to show weaker antimicrobial activities than the parent peptide (Tamamura et al., 1993a). Acyclization of gramicidin S (Erlanger & Goode, 1954, 1959) and related peptides (Makisumi et al., 1971a,b; Satoh et al., 1990) significantly reduces their potencies. Thus, we synthesized a linear tachyplesin I derivative (T-Acm) in which the four SH groups of tachyplesin I were protected with Acm (acetamidomethyl) groups (Figure 1). In this report, we compare the interactions of T-Acm and T-SS with lipid bilayers in terms of the membrane-permeabilization activity, the intramembrane location of Trp^2, and the bilayer-micellization ability. Furthermore, the molecular aspects of these interactions will be discussed on the basis of the data obtained by use of the Fourier transform infrared polarized attenuated total reflection (FTIR-PATR) technique.

Lys-Trp-Cys-Phe-Arg^5-Val-Cys-Tyr-Arg
| | |
NH_2-Arg-Cys-Arg^{15}-Arg-Tyr-Cys-Ile-Gly^{10}

Lys-Trp-Cys-Phe-Arg^5-Val-Cys-Tyr-Arg-Gly^{10}-Ile-Cys-Tyr-Arg-Arg^{15}-Cys-Arg-NH_2
| | | |
Acm Acm Acm Acm

FIGURE 1: Structures of T-SS (top) and T-Acm (bottom).

MATERIALS AND METHODS

Materials. T-SS and T-Acm were synthesized by Fmoc-based solid-phase synthesis and ascertained as described elsewhere (Akaji et al., 1989). The synthesized peptides were initially purified by RP-HPLC and then were further refined by gel filtration (Sephadex G-15, 2.5 × 35 cm column, with 0.02 M HCl being used as an eluent) followed by lyophilization. The purities (ca. 100%) were determined by quantitative amino acid analysis.

Egg yolk L-α-phosphatidylcholine (PC) was purchased from Sigma. L-α-Phosphatidylglycerol (PG), which was enzymatically converted from PC, was a gift from Nippon Fine Chemical Co. (Takasago, Japan). Calcein and spectroscopy

* Abstract published in *Advance ACS Abstracts*, October 1, 1993.

[1] Abbreviations: T-SS, tachyplesin I; T-Acm, an acyclic tachyplesin I analog with the four SH groups of tachyplesin I protected by acetamidomethyl groups; NMR, nuclear magnetic resonance; FTIR-PATR, Fourier transform infrared polarized attenuated total reflection; RP-HPLC, reversed-phase high-performance liquid chromatography; CD, circular dichroism; PC, egg yolk L-α-phosphatidylcholine; PG, L-α-phosphatidylglycerol enzymatically converted from PC; LUVs, large unilamellar vesicles.

0006-2960/93/0432-11704$04.00/0

grade organic solvents were provided by Dojindo Laboratory (Kumamoto, Japan). All other chemicals from Wako (Tokyo, Japan) were of special grade. A Tris buffer (10 mM Tris-HCl/150 mM NaCl/1 mM EDTA, pH 7.0) was prepared with twice-distilled water from a glass still.

Leakage from LUVs. Large unilamellar vesicles (LUVs) were prepared by an extrusion method and characterized as described elsewhere (Matsuzaki et al., 1991b,c). Briefly, a lipid film was hydrated with a 70 mM calcein solution (pH 7.0). The suspension was vortexed and freeze-thawed for five cycles, followed by successive extrusion through polycarbonate filters (a filter of 0.6-μm pore size, 5 times, and doubly stacked filters of 0.1-μm pore size, 10 times) using an extruder (Lipex Biomembranes Inc.). Untrapped calcein was removed by gel filtration (Sephadex G-50 medium, 1.5 × 30 cm column, with the buffer being used as an eluent). The separated LUV fraction was diluted appropriately with the buffer. The lipid concentration was determined by phosphorus analysis (Bartlett, 1959).

The LUV suspension was mixed with a peptide/buffer solution in a cuvette with stirring. The leakage of calcein out of the LUVs was monitored by measuring the fluorescence intensity at 520 nm (excited at 490 nm) on a Shimadzu RF-5000 spectrofluorometer (Allen & Cleland, 1980). The fluorescence intensity corresponding to 100% leakage was determined by adding a 10%, w/v, Triton X-100 solution (20 μL) to 2 mL of the sample.

Trp Fluorescence. Fluorescence spectra of the Trp residue of T-SS or T-Acm (5 μM in the Tris buffer, excited at 280 nm) were measured during the titration of the peptide solution with small aliquots of a PG LUV suspension (36 mM) in a cuvette. Fluorescence spectra were corrected according to Melhuish's method (Melhuish, 1962) after subtraction of the corresponding blank spectra.

Fluorescence quenching was studied as follows: An LUV suspension was mixed with a peptide/buffer solution (final concentration 5 μM) in a cuvette (2 mL). Fluorescence intensities (at 350 nm in the absence of the LUVs and at 336 nm in the presence of the LUVs, both excited at 280 nm) were recorded during the titration of the solution with small aliquots of a 5 M acrylamide/buffer solution in the cuvette. The inner filter effects due to absorption of the excitation beam by acrylamide were corrected (De Kroon et al., 1990).

Micellization. The time course of micellization was followed by measuring the 90° light scattering intensity. A PG LUV suspension (final concentration 7.5 μM) was mixed with a peptide/buffer solution (final concentration 1.4 μM, L/P = 5) or with the buffer (control) in a cuvette at zero time. The 90° light scattering intensity at 400 nm was monitored under gentle stirring on the spectrofluorometer. The micelle-like particles formed were examined by negative-stain electron microscopy. A PG LUV suspension was incubated for 1 h with T-SS or T-Acm at an L/P value of 7. The sample was negatively stained with a 1.5%, w/v, ammonium molybdate solution (pH 6.0) and then cast onto carbon–collodion grids, followed by air drying. Transmission electron micrographs were taken on a Hitachi H-500 electron microscope at 75 kV.

FTIR-PATR Spectroscopy. Dry-cast films of PG or PG/peptide (40/1, mol/mol) were prepared by uniformly spreading a chloroform/methanol solution of PG (10 μmol) or PG (10 μmol)/peptide (0.25 μmol) on one face of a germanium ATR plate (52 × 18 × 2 mm) followed by gradual evaporation of the solvent. The film thickness estimated from the applied amount of the lipid was about 8 μm. The lipid film was hydrated under a stream of D_2O-saturated N_2 gas for more than 20 h to achieve complete hydration. The amount of hydrated water (greater than 30%, w/w) was estimated on the basis of the absorbance ratio of the O–D stretching band to the methylene antisymmetric stretching band of the lipid (Okamura et al., 1990). The spectra were recorded on a Nicolet 205 FTIR spectrophotometer equipped with an Hg–Cd–Te detector at ambient temperatures (25 ± 3 °C). To minimize spectral contributions of atmospheric water vapor, the instrument was purged with dry N_2 gas. PATR measurements were carried out using a Perkin-Elmer multiple ATR attachment and a Specac KRS-5 polarizer. The angle of incidence was 45°, and the number of total reflections was 12 on the film side. The 256 interferograms that were collected had a resolution of 4 cm^{-1} and were analyzed by use of Nicolet SX software on a Nicolet 620 workstation. The subtraction of the gently sloping water vapor bands was carried out to improve the background prior to the frequency measurement. The accuracy of the frequency reading was better than ±0.1 cm^{-1}. The dichroic ratio, R, defined by $\Delta A_{\parallel}/\Delta A_{\perp}$, was calculated from the polarized spectra. The absorbance (ΔA) was obtained as the peak height of each absorption band. The subscripts $\parallel$ and $\perp$ refer to polarized light with its electric vector parallel and perpendicular to the plane of incidence, respectively. The base-line method was used to minimize the background artifact.

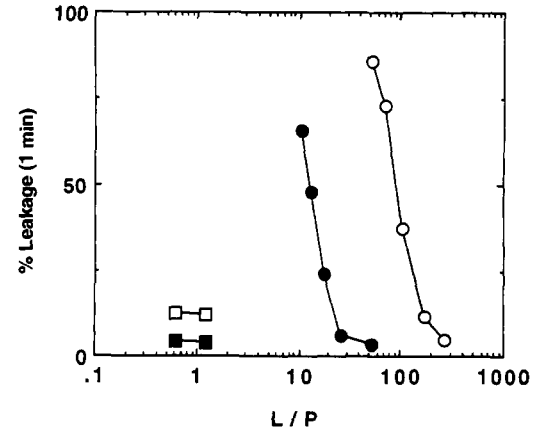

FIGURE 2: Peptide-induced membrane permeabilization at 30 °C. The percent leakage of calcein from LUVs for the initial minute is plotted as a function of the lipid to peptide molar ratio, L/P. Peptide: open symbols, T-SS; closed symbols, T-Acm. Lipid: circles, PG; squares, PC. The lipid concentration was 5–7 μM.

RESULTS

Permeabilization of Lipid Bilayers. Figure 2 shows the peptide-induced permeabilization of lipid bilayers composed of PG or PC, as estimated by leakage of the fluorescent dye calcein trapped within vesicles. The calcein efflux implies the formation of a structural defect or a pore through which the relatively large dye molecule can pass (Matsuzaki et al., 1989b). Both peptides permeabilized the acidic membranes much more strongly than the electrically neutral bilayers, suggesting the importance of electrostatic interactions between the positively charged peptides and the negatively charged lipids. The cyclic T-SS peptide caused the dye leakage at L/P values 1 order of magnitude larger than those for the linear T-Acm peptide, which coincides with the stronger antimicrobial activity of the former (Tamamura et al., 1993a).

Trp Fluorescence. Fluorescence of the Trp[2] residue was utilized to estimate peptide binding to membranes and the intramembrane Trp location. Figure 3 illustrates changes in the fluorescence maximal wavelength (a) and intensity (b)

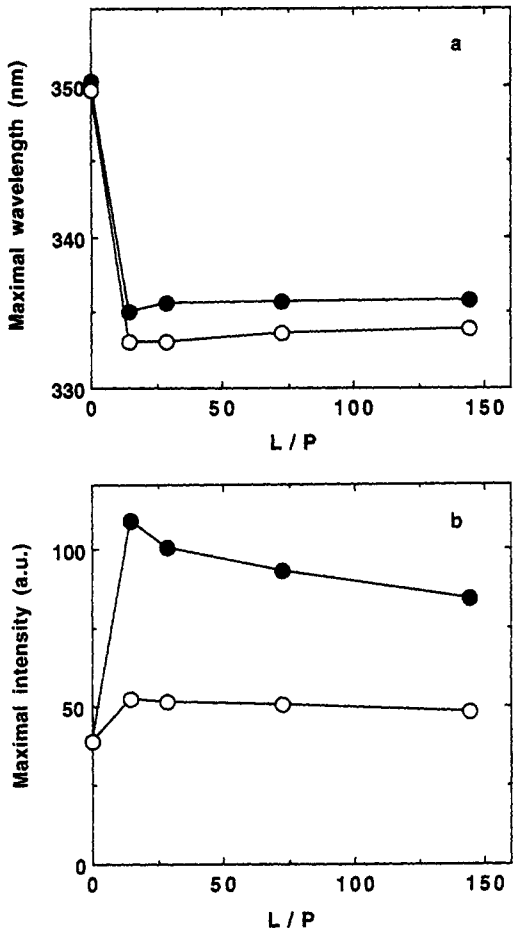

FIGURE 3: Fluorescence spectral changes of the peptide Trp residues upon membrane binding at 30 °C. A peptide/buffer solution (5 μM) was titrated with a concentrated PG LUV suspension. Maximal wavelength (a) or intensity (b) is plotted as a function of the lipid to peptide molar ratio, L/P. Peptide: open symbols, T-SS; closed symbols, T-Acm. Excited at 280 nm.

upon membrane binding. A buffer solution of each peptide was titrated with a concentrated PG LUV suspension. To avoid possible morphological changes of the vesicles (Matsuzaki et al., 1993), the titration was started at an L/P ratio of 14. Addition of the lipid caused a blue shift from 350 to 333–336 nm (Figure 3a) and an enhanced intensity (Figure 3b), indicating that the Trp residues are located in a hydrophobic environment in the bilayers. The membrane binding affinities of both T-SS and T-Acm, which have the same net charge, appear to be equally significantly strong, because an L/P ratio of 14 was sufficient to attain maximal spectral changes. We have confirmed the very strong binding of T-SS elsewhere (Matsuzaki et al., 1991c). The apparent binding constant was greater than 10^7 M^{-1}. We could not quantitatively compare the binding affinities, because their exact determination would require experiments at much lower L/P ratios where the integrity of the bilayer is lost (Matsuzaki et al., 1993). At lower L/P ratios, the Trp fluorescence of both peptides, especially that of T-Acm, was much more intense (Figure 3b) and blue-shifted (Figure 3a). This may result from optical artifacts because of light scattering. To check this possibility, we estimated the effects of light scattering on fluorescence spectra of indoxy sulfate (excited at 280 nm), which is expected to have no interactions with the PG vesicles because of electrostatic repulsions. The presence of 1 mM lipid, which showed an OD value as high as 0.43 at the excitation wavelength, *never* affected the fluorescence spectra after the corresponding blank was subtracted (data not shown).

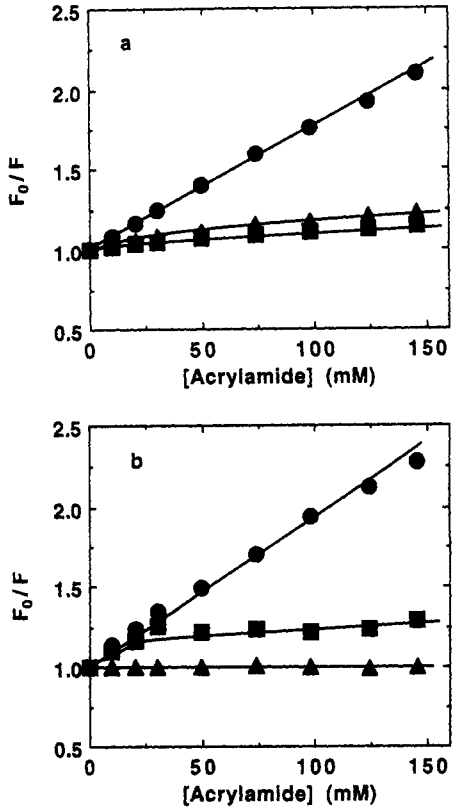

FIGURE 4: Stern–Volmer plots for fluorescence quenching of the peptide Trp residues by acrylamide at 30 °C: (a) T-Acm; (b) T-SS. PG to peptide molar ratios: circles, 0; squares, 23; triangles, 232. The peptide concentration was 5 μM. Excited at 280 nm. Inner filter effects due to acrylamide absorption have been corrected (see text).

The intramembrane location of Trp[2] was further inferred on the basis of fluorescence quenching by an aqueous quencher, acrylamide. Figure 4a depicts the Stern–Volmer plot for T-Acm. In the absence of PG vesicles, the Trp fluorescence was quenched with a Stern–Volmer constant of 7.5 M^{-1}, which is similar to the value of 8.7 M^{-1} found for T-SS (Figure 4b). In the presence of the vesicles, only a slight quenching was observed even at the highest acrylamide concentration (145 mM), i.e., ca. 15% and 23% at L/P ratios of 23 and 232, respectively. The different quenching is not assignable to the contributions from any highly quenched free peptide fluorescence, because the free peptide fraction, which itself is considered to be rather small (Matsuzaki et al., 1991c), should be larger at the lower L/P ratio. For T-SS, the Trp residue is completely shielded from the aqueous quencher at an L/P value of 232 (Figure 4b). In contrast, at an L/P value of 23, moderate quenching was observed. This might be explained by assuming that the free peptide fraction was as much as 0.5, which is contrary to the observed high membrane affinity (Matsuzaki et al., 1991c). Thus, the quenching is not ascribable to the free peptide. Peptide-induced membrane permeabilization (Figure 2) may allow the aqueous quencher to contact the membrane-embedded Trp residue.

Micellization. Figures 5 and 6 compare the micellization ability of T-SS and T-Acm at relatively low L/P values. The relative 90° light scattering intensity of T-SS-treated PG LUVs gradually decreased below unity after soaring temporarily (Figure 5), thus indicating vesicular aggregation and/or fusion followed by micellization (Matsuzaki et al., 1993). In the case of T-Acm, the disintegration of the larger particles proceeded more slowly; however, the aggregation and/or fusion appeared to occur more rapidly. Electron micrographs (Figure

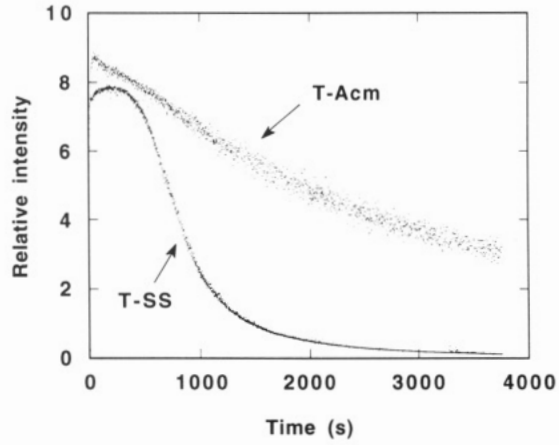

FIGURE 5: Time course of peptide-induced morphological changes of PG LUVs at 30 °C. The 90° light scattering intensity (at 400 nm) of peptide-treated LUVs (L/P = 5) relative to that of the control (peptide-untreated LUVs) is plotted against the incubation time.

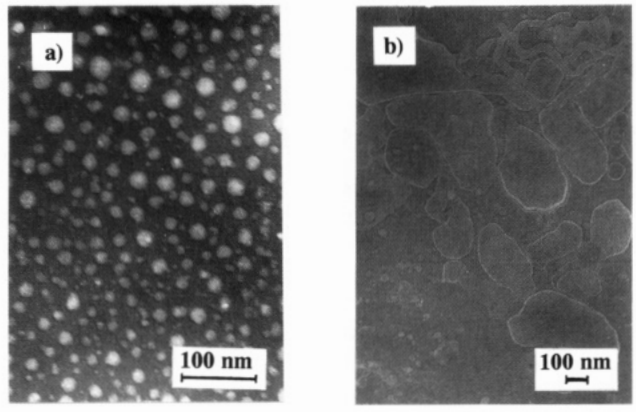

FIGURE 6: Negative-stain electron micrographs of tachyplesin–lipid micelles. A PG LUV suspension was incubated for 1 h with T-SS (a) or T-Acm (b) at an L/P value of 7.

6) clearly depict complete micellization (micelles 10–20 nm in diameter) of the LUVs that were incubated with T-SS, whereas the coexistence of micelles and their precursors, i.e., fused large vesicles, was observed for the T-Acm-treated vesicles. These data demonstrate the stronger micellization activity of the cyclic peptide.

FTIR-PATR. FTIR spectroscopy is a useful tool for investigating peptide–lipid interactions, because conformations of functional groups of both peptides and lipids can be estimated simultaneously and without perturbation (Amey & Chapman, 1984; Casal & Mantsch, 1984; Mendelsohn et al., 1984; Byler & Susi, 1986; Arrondo et al., 1993). The PATR technique enables us to evaluate molecular orientations (Fringeli & Fringeli, 1979; Fringeli & Günnthard, 1981; Okamura et al., 1986, 1990; Brauner et al., 1987; Cabiaux et al., 1989; Cornell et al., 1989; Wald et al., 1990; Matsuzaki et al., 1991a; Frey & Tamm, 1991).

Amide I′ band contours in the wavenumber range of 1600–1700 cm^{-1} are well known to be diagnostic of protein secondary structures [for review, see Byler and Susi (1986) and Arrondo et al. (1993)]. Figure 7 shows the FTIR-PATR spectra in this region of PG/peptide D_2O-hydrated films at an L/P value of 40. Both spectra was characteristic of antiparallel β-sheet conformations (Miyazawa, 1960; Byler & Susi, 1986; Surewicz et al., 1987; Arrondo et al., 1993). That is, an intense band at 1620–1630 cm^{-1} combined with a weak band near 1685 cm^{-1} was observed. The former absorption corresponds to the $\nu(\pi,0)$ transition with its transition moment along the

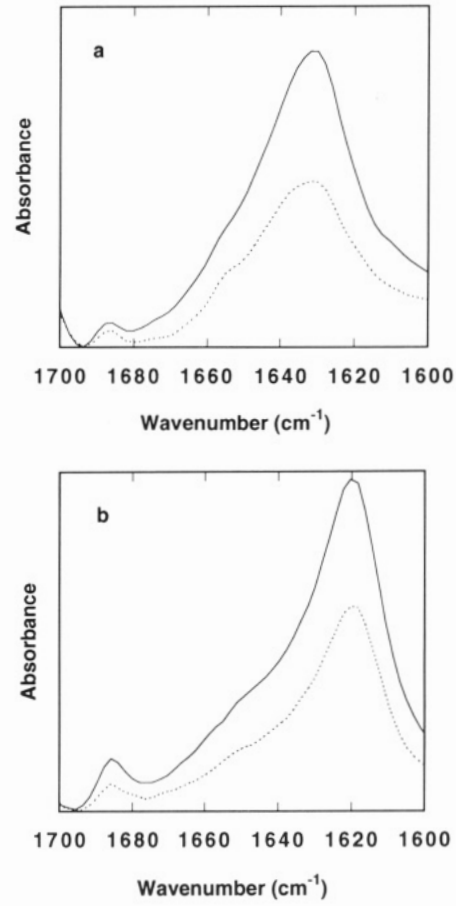

FIGURE 7: The amide I′ region of the FTIR-PATR spectra of D_2O-hydrated PG/T-SS (a) and PG/T-Acm films (b) at an L/P value of 40. Solid and dotted lines refer to the IR beam with its electric vector parallel and perpendicular to the plane of incidence, respectively.

intersection of two adjacent peptide planes. The latter band is due to the $\nu(0,\pi)$ transition whose moment is toward the fiber axis. The dichroic ratio, R, of an absorption band is a measure of the orientation of its transition moment or its molecular axis. For membranes much thicker ($\sim$8 μm) than the penetration depth (under our experimental conditions, 0.2–0.8 μm in the range 3000–800 cm^{-1}), and R value smaller than 2 indicates that the moment lies essentially parallel to the membrane surface (Matsuzaki et al., 1991a). Inspection of Figure 7a revealed that, in the case of T-SS, both the $\nu(\pi,0)$ and $\nu(0,\pi)$ transition moments, which are in the plane of the β-sheet, lie parallel to the membrane surface, because the R values were 1.8 ± 0.1 and 1.2 ± 0.2 (n = 3), respectively. Figure 7b depicts that T-Acm seems to have a similar parallel orientation. (The R values were 1.6 ± 0.0 and 1.9 ± 0.1 (n = 2), respectively.)

Peptide-induced disruption of bilayer structures was estimated by examining the CH_2 symmetric stretching band near 2853 cm^{-1}, which is less affected by protein-related absorptions compared to the more intense, antisymmetric stretching band around 2923 cm^{-1} (Casal & Mantsch, 1984). Table I summarizes the frequency and the order parameter, S, of the lipid hydrocarbon chain calculated from the dichroic ratio of the former band by use of eq 1 (Matsuzaki et al., 1991a).

$$S = -2(R - 2)/(R + 1.45) \quad (1)$$

This parameter is connected to the mean orientational angle, α, between the hydrocarbon chain and the membrane normal through eq 2, assuming the uniaxial orientation of the chain

Table I: Conformations and Orientations of Lipid Hydrocarbon Chains

sample[a]	n^b	frequency (cm^{-1})[c]	order parameter[c,d]
PG	3	2852.9 ± 0.2	0.45 ± 0.04
PG/T-SS	3	2852.9 ± 0.2	0.33 ± 0.10
PG/T-Acm	2	2852.7 ± 0.1	0.18 ± 0.05

[a] Samples were hydrated with D_2O vapor. The lipid to peptide molar ratio was 40. [b] Number of experiments. [c] For the CH_2 symmetric stretching band. Average ± SD. [d] Calculated by use of eq 1.

around the normal.

$$S = (1/2)[(3\ cos^2\ \alpha) - 1] \quad (2)$$

The frequency, a measure of the trans/gauche conformer ratio (Casal & Mantsch, 1984), was never affected by incorporation of both peptides. In contrast, the presence of the tachyplesin peptides reduced the order parameter, indicating that the orientational axis of the lipid per se was inclined. Surprisingly, the linear T-Acm, the weaker membrane permeabilizer (Figure 2), caused a much more significant decrease in S, i.e., a far more serious membrane disruption.

DISCUSSION

Acyclization of membrane-acting cyclic peptides generally reduces their potencies (Erlanger & Goode, 1954, 1959; Makisumi et al., 1971a,b; Satoh et al., 1990; Tamamura et al., 1993a). However, the detailed mechanisms are still unknown. Elucidation of the effects of the cyclic structure on the peptide–membrane interactions would allow us to better understand their molecular mechanisms. Tachyplesin has two S–S bonds (Figure 1). To fully elucidate the role of the disulfide bridges, we have to examine two additional peptides, the first having a disulfide bond between Cys^3 and Cys^{16} only and the second possessing an S–S bond between Cys^7 and Cys^{12}. Our recent results demonstrated that the former exhibits antiviral activity and cytotoxicity similar to those of the parent tachyplesin I, whereas linear analogs show much weaker potencies (Masuda et al., 1992; Tamamura et al., 1993a). Thus, as the first step, we compared the differences between T-SS and T-Acm in terms of their interactions with their final targets, i.e., membranes, by employing fluorescence and FTIR spectroscopy.

Fluorescence. Trp fluorescence has been widely used to obtain molecular details of peptide–lipid interactions (De Kroon et al., 1990; Matsuzaki et al., 1991c; Chung et al., 1992). Spectral properties are sensitive to the environment. Quenching techniques enable us to infer the intramembrane locations of peptides. In the buffer, the maximal wavelengths of both Trp residues were about 350 nm (Figure 3a), typical of Trp in an aqueous environment and in accordance with effective quenching by a water-soluble quencher, acrylamide (Figure 4). The Stern–Volmer constants (7.5 M^{-1} for T-Acm and 8.7 M^{-1} for T-SS) are somewhat smaller but comparable with smaller peptides (12–17 M^{-1}; De Kroon et al., 1990). Thus, in the absence of membranes, the Trp residues of both peptides are exposed to the aqueous medium. Spectral changes upon membrane binding (Figure 3) indicate that both Trp residues are embedded in a hydrophobic region of the bilayers. Shielding from the aqueous quencher (Figure 4) argues for this conclusion. The Trp^2 residue of T-Acm appears to be buried more deeply in the hydrophobic region at lower L/P values, as judged from its greater blue shift, its intense fluorescence (Figure 3), and its reduced quenching (Figure 4), partly because the peptide-induced membrane disruption (Table I) enables the Trp residue to penetrate more deeply into the membrane. Similarly, the maximal wavelength (Figure 3a) and the quenching data (Figure 4) suggest that the Trp^2 residue of the linear peptide is located closer to the membrane surface compared to that of the cyclic peptide, at least for an L/P value of 232. We have revealed (Matsuzaki et al., 1991c) that the latter is buried in a hydrophobic region near the membrane surface; however, the quantum yield in the membrane was greater for T-Acm (Figure 3b). Park et al. (1992) reported that, upon membrane binding, T-SS appears to undergo a conformational change, which may bring the Trp side chain closer to the adjacent S–S bond, a fluorescence quencher (Cowgill, 1967), resulting in a reduced fluorescence intensity compared to that of T-Acm.

FTIR-PATR. We carried out FTIR-PATR experiments to elucidate the molecular aspects of the peptide–lipid interactions. We examined the amide I′ bands of the peptides and the CH_2 symmetric stretching band of the lipid. The amide I′ band is approximated to be the C=O stretching vibration. The band contour is diagnostic of protein secondary structures which lead to characteristic intrachain and interchain interactions between amide groups. This problem was theoretically treated by use of the first-order perturbation theory (Miyazawa, 1960). According to this treatment, the observed intense bands in the range 1620–1630 cm^{-1} and the weak bands around 1685 cm^{-1} (Figure 7) can be assigned to the $\nu(\pi,0)$ and $\nu(0,\pi)$ transitions of antiparallel β-sheet structures. The lower frequency of the former band of the linear peptide (ca. 1620 cm^{-1}) compared to that of the cyclic peptide (ca. 1630 cm^{-1}) indicates a stronger interchain hydrogen bonding of T-Acm (Surewicz et al., 1987). Estimation of the sheet plane orientations requires the dichroic ratios of both the $\nu(\pi,0)$ and the $\nu(0,\pi)$ bands, whose transition moments lie in the sheet plane and are perpendicular to each other (Miyazawa, 1960). The angles between these transition moments and the bilayer normal are denoted by a and b for the $\nu(\pi,0)$ and $\nu(0,\pi)$ transitions, respectively. Assuming the uniaxial orientation (Matsuzaki et al., 1991a), the order parameter, S_a or S_b, defined by equations similar to eq 2, can be estimated by eq 3.

$$S_a\ (\text{or}\ S_b) = (R - 2)/(R + 1.45) \quad (3)$$

The order parameter of the sheet normal, S_c, can be evaluated by use of the following relation:

$$S_a + S_b + S_c = 0 \quad (4)$$

The calculated S_c values were ~0.37 and ~0.16 for T-SS and T-Acm, respectively, although these estimates may contain some errors because of the weak overlapping features of the $\nu(0,\pi)$ bands. The positive S_c values imply that the sheet normals are essentially perpendicular to the plane of the Ge plate. The order parameter of the gramicidin helix, which is known to span the bilayer, is reported to be 0.58 in dimyristoylphosphatidylcholine membranes (Okamura et al., 1986). In contrast, melittin, which orients parallel to the membrane surface, has S values of –0.3 to –0.5 in fully hydrated liquid-crystalline bilayers (Frey & Tamm, 1991). Strikingly, our S_c values are in good agreement with the order parameters of the lipid hydrocarbon chain, S (Table I). Thus, we can conclude that the antiparallel β-sheets of both peptides lie parallel to the membrane surface with their hydrophobic surfaces slightly penetrating the hydrophobic region of the bilayer. This conclusion is consistent with the surface locations of the Trp^2 residues (Figure 4).

Peptide-induced membrane permeabilization has often been explained in terms of disruption of the bilayer lipid organization

(Terwilliger et al., 1982; Matsuzaki et al., 1991a; Ostolaza et al., 1993). The different membrane-perturbing activities of two peptaibols, hypelcin A and trichopolyn I, can be well explained in terms of different disruptions of the lipid organization, as revealed by the FTIR-PATR technique (Matsuzaki et al., 1991a). Thus, we examined the lipid order by use of this technique (Table I). The S value in the absence of the peptides (0.45) is typical of bilayers in the liquid-crystalline state (Okamura et al., 1990; Frey & Tamm, 1991). Incorporation of T-SS slightly reduced the order parameter, whereas the binding of T-Acm, the less potent membrane permeabilizer, caused more significant membrane disruption. It should be noted (see Figure 2) that the L/P value employed here (40) is smaller than the L/P values at which leakage occurs for T-SS (60–250) but larger than those for T-Acm (10–30). Therefore, under membrane-permeabilizing conditions, the membrane organization will be less perturbed for T-SS but much more disrupted for T-Acm.

Comparison between T-SS and T-Acm. Both peptides, T-SS and T-Acm, possess several common properties. First, they demonstrate acidic lipid specificity (Figure 2). Similar observations have been reported for magainin 1, a highly basic, helical peptide from the skin of an African frog (Matsuzaki et al., 1989a). Weak interactions with the zwitterionic lipid may be attributed to the high water solubility (low membrane partitioning) and intramembrane interpeptide repulsions, because of the large positive charge (+7), which instead endows the peptides with equally strong affinities for negatively charged bilayers (Figure 3). Second, the tachyplesin peptides have antiparallel β-sheet structures in membranes (Figure 7). NMR (Kawano et al., 1990; Tamamura et al., 1993b) and CD (Tamamura et al., 1993a) studies indicate that in aqueous solutions T-SS also conforms to a cyclic antiparallel β-sheet structure with a type II β-turn, whereas T-Acm conforms to an unordered structure. Most constituent amino acids (Val, Ile, Tyr, Cys, Trp) highly favor β-sheet structures, and Arg is never a β-sheet breaker (Chou & Fasman, 1974). Furthermore, the amino acid sequence contains three tandem repeats of the tetrapeptide [hydrophobic amino acid]-Cys-[hydrophobic amino acid]-Arg. Thus, the primary structure of tachyplesin I is designed to potentially form an amphiphilic β-sheet conformation capable of interacting with membranes. The FTIR-PATR experiments (Figure 7) revealed that the β-sheets lie parallel to the membrane surface, as expected from their amphiphilic characters. Synthetic peptides designed to form amphiphilic β-sheet structures have been shown to interact with lipid bilayers without deep penetration (Ono et al., 1990).

In spite of these similarities, the cyclic peptide much more effectively induces membrane permeabilization compared to the linear variant (Figure 2; Park et al., 1992), in keeping with the stronger antimicrobial activity of the former (Tamamura et al., 1993a). The observation that the linear T-Acm, the weaker membrane permeabilizer, produced a far more serious membrane disruption (Table I) suggests the possibility that the mechanisms of membrane permeabilization by the cyclic peptide are completely different from those by the linear peptide. For elucidating the antimicrobial mechanisms, it is helpful to compare these results with the membrane permeabilization induced by gramicidin S, an antibacterial cyclic amphiphilic β-sheet decapeptide, which is known to disrupt lipid organization (Susi et al., 1979). Our recent data (K. Matsuzaki et al., unpublished work) indicate that the peptide caused the leakage of calcein from PG LUVs at L/P ratios around 5, which are comparable with those of T-Acm (Figure 2), taking into account the molecular size difference. The order parameter of the lipid acyl chain at an L/P value of 20 was around 0.2, very similar to the value observed for T-Acm (Table I). Thus, T-Acm and gramicidin S may have similar mechanisms for membrane permeabilization, i.e., perturbation of the lipid organization, just like the "wedge effect" (Terwilliger et al., 1982). Then how does T-SS enhance the membrane permeability without significantly perturbing the bilayer? We have already reported that the permeabilization is not due to micellization (Matsuzaki et al., 1993), although this mechanism will also work when the vesicles are exposed to a high concentration of the peptide. One possibility is that the cyclic peptide forms a transmembrane channel-like pore. The length of the T-SS molecule (about 30 Å) is sufficient to withstand this perpendicular orientation. Our preliminary study showed that tachyplesin I induced an anion-selective current in planar lipid bilayers, whereas T-Acm did not. Such a channel would be expected to yield a much smaller S_c value, if it is sufficiently stable. However, the life span of the pore is rather short (<15 ms), on the basis of the "gradual" leakage mode (Matsuzaki et al., 1993). This suggests that most peptide molecules, lying parallel to the membrane surface as revealed by FTIR-PATR, sometimes take a short-lived "open form" by fluctuation. A Leu-rich peptide with amphiphilic β-sheet conformations that forms a channel-like pore in membranes has been reported (Krantz et al., 1991). The confirmation of the channel formation is in progress.

The fluorescence study (Figures 3 and 4) suggested that the Trp residue of T-Acm is located somewhat closer to the membrane surface compared to that of T-SS. Apparently this observation is inconsistent with the more significant membrane disruption induced by the linear peptide. However, it should be noted that, in the wedge effect (Terwilliger et al., 1982), the peptide occupies space near the *head group* region of the phospholipid bilayer, but does *not* extend all the way to the center of the bilayer. Furthermore, the perturbation of the lipid organization may change the microenvironments around the Trp residues.

The tachyplesin peptides cause not only membrane permeabilization but also vesicular aggregation, fusion, and micellization at lower L/P values (Figures 5 and 6; Matsuzaki et al., 1993), even though the mechanisms and the detailed micelle structures are not known. Although these morphological changes may not be directly related to the membrane perturbation, it is of general interest to compare the activity of the two peptides. The aggregation–fusion step proceeds more rapidly in the case of T-Acm (Figure 5), partly because its flexible linear chain can effectively bridge adjacent vesicles. The interchain hydrogen bonds (vide supra) will contribute to the formation of this type of larger suprastructure. The stronger membrane perturbation (Table I) by the peptide may also be responsible for this observation. In contrast, T-SS more strongly promotes the disintegration of fused vesicles into smaller micelle-like particles. If the micelles were spherical, an electrically neutral hydrophobic compact core would be effectively formed by the cyclic T-SS and the lipids; if they were disklike, the periphery would be efficiently covered by T-SS molecules capable of spanning the bilayer. Elucidation of micelle structures is a subject of continuing study.

In summary, the linear T-Acm peptide appears to permeabilize lipid bilayers through a membrane disruption mechanism, while the cyclic T-SS peptide more effectively enhances membrane permeability without affecting lipid organization. The elucidation of the detailed mechanism is a subject of continuing study.

ACKNOWLEDGMENT

We are grateful to Prof. J. Seelig (Biocenter of the University of Basel) for helping us with the revision of the manuscript. We also thank Nippon Fine Chemical Co. for their kind gift of PG.

REFERENCES

Akaji, K., Fujii, N., Tokunaga, F., Miyata, T., Iwanaga, S., & Yajima, H. (1989) *Chem. Pharm. Bull. 37*, 2661–2664.

Allen, T. M., & Cleland, L. G. (1980) *Biochim. Biophys. Acta 597*, 418–426.

Amey, R. L., & Chapman, D. (1984) in *Biomembrane Structure and Function* (Chapman, D., Ed.) pp 199–256, Verlag Chemie, Weinheim.

Arrondo, J. L. R., Muga, A., Castresana, J., & Goñi, F. M. (1993) *Prog. Biophys. Mol. Biol. 59*, 23–56.

Bartlett, G. R. (1959) *J. Biol. Chem. 234*, 466–468.

Brauner, J. W., Mendelsohn, R., & Prendergast, F. G. (1987) *Biochemistry 26*, 8151–8158.

Byler, D. M., & Susi, H. (1986) *Biopolymers 25*, 469–487.

Cabiaux, V., Brasseur, R., Wattiez, R., Falmagne, P., Ruysschaert, J.-M., & Goormaghtigh, E. (1989) *J. Biol. Chem. 264*, 4928–4938.

Casal, H. L., & Mantsch, H. H. (1984) *Biochim. Biophys. Acta 779*, 381–401.

Chou, P. Y., & Fasman, G. D. (1974) *Biochemistry 13*, 222–244.

Chung, L. A., Lear, J. D., & DeGrado, W. F. (1992) *Biochemistry 31*, 6608–6616.

Cornell, D. G., Dluhy, R. A., Briggs, M. S., McKnight, C. J., & Gierasch, L. M. (1989) *Biochemistry 28*, 2789–2797.

Cowgill, R. W. (1967) *Biochim. Biophys. Acta 37*, 37–44.

De Kroon, A. I. P. M., Soekarjo, M. W., DeGier, J., & De Kruijff, B. (1990) *Biochemistry 29*, 8229–8240.

Erlanger, B. F., & Goode, L. (1954) *Nature 174*, 840–841.

Erlanger, B. F., & Goode, L. (1959) *Science 131*, 669–670.

Frey, S., & Tamm, L. K. (1991) *Biophys. J. 60*, 922–930.

Fringeli, U. P., & Fringeli, M. (1979) *Proc. Natl. Acad. Sci. U.S.A. 76*, 3852–3856.

Fringeli, U. P., & Günnthard, H. H. (1981) in *Membrane Spectroscopy* (Grell, E., Ed.) pp 270–332, Springer-Verlag, Berlin.

Kawano, K., Yoneya, T., Miyata, T., Yoshikawa, K., Tokunaga, F., Terada, Y., & Iwanaga, S. (1990) *J. Biol. Chem. 265*, 15365–15367.

Krantz, D. D., Zidovetzki, R., Kagan, B. L., & Zipursky, S. L. (1991) *J. Biol. Chem. 266*, 16801–16807.

Makisumi, S., Matsuura, S., Waki, M., & Izumiya, N. (1971a) *Bull. Chem. Soc. Jpn. 44*, 210–214.

Makisumi, S., Waki, M., & Izumiya, N. (1971b) *Bull. Chem. Soc. Jpn. 44*, 143–148.

Masuda, M., Nakashima, H., Ueda, T., Naba, H., Ikoma, R., Otaka, A., Terakawa, Y., Tamamura, H., Ibuka, T., Murakami, T., Koyanagi, Y., Waki, M., Matsumoto, A., Yamamoto, N., Funakoshi, S., & Fujii, N. (1992) *Biochem. Biophys. Res. Commun. 189*, 845–850.

Matsuzaki, K., Harada, M., Handa, T., Funakoshi, S., Fujii, N., Yajima, H., & Miyajima, K. (1989a) *Biochim. Biophys. Acta 981*, 130–134.

Matsuzaki, K., Nakai, S., Handa, T., Takaishi, Y., Fujita, T., & Miyajima, K. (1989b) *Biochemistry 28*, 9392–9398.

Matsuzaki, K., Shioyama, T., Okamura, E., Umemura, J., Takenaka, T., Takaishi, Y., Fujita, T., & Miyajima, K. (1991a) *Biochim. Biophys. Acta 1070*, 419–428.

Matsuzaki, K., Takaishi, Y., Fujita, T., & Miyajima, K. (1991b) *Colloid Polym. Sci. 269*, 604–611.

Matsuzaki, K., Fukui, M., Fujii, N., & Miyajima, K. (1991c) *Biochim. Biophys. Acta 1070*, 259–264.

Matsuzaki, K., Fukui, M., Fujii, N., & Miyajima, K. (1993) *Colloid Polym. Sci.*, in press.

Melhuish, W. H. (1962) *J. Opt. Soc. Am. 52*, 1256–1258.

Mendelsohn, R., Anderle, G., Jaworsky, M., Mantsch, H. H., & Dluhy, R. A. (1984) *Biochim. Biophys. Acta 775*, 215–224.

Miyazawa, T. (1960) *J. Chem. Phys. 32*, 1647–1652.

Nakamura, T., Furunaka, H., Miyata, T., Tokunaga, F., Muta, T., Iwanaga, S., Niwa, M., Takao, T., & Shimonishi, Y. (1988) *J. Biol. Chem. 263*, 16709–16712.

Ohta, M., Ito, H., Masuda, K., Tanaka, S., Arakawa, Y., Wacharotayankun, R., & Kato, N. (1992) *Antimicrob. Agents Chemother. 36*, 1460–1465.

Okamura, E., Umemura, J., & Takenaka, T. (1986) *Biochim. Biophys. Acta 856*, 68–75.

Okamura, E., Umemura, J., & Takenaka, T. (1990) *Biochim. Biophys. Acta 1025*, 94–98.

Ono, S., Lee, S., Mihara, H., Aoyagi, H., Kato, T., & Yamasaki, N. (1990) *Biochim. Biophys. Acta 1022*, 237–244.

Ostolaza, H., Bartolomé, B., de Zárate, I. O., de la Cruz, F., & Goñi, F. M. (1993) *Biochim. Biophys. Acta 1147*, 81–88.

Park, N. G., Lee, S., Oishi, O., Aoyagi, H., Iwanaga, S., Yamashita, S., & Ohno, M. (1992) *Biochemistry 31*, 12241–12247.

Satoh, K., Okuda, H., Horimoto, H., Kodama, H., & Kondo, M. (1990) *Bull. Chem. Soc. Jpn. 63*, 3467–3472.

Surewicz, W. K., Mantsch, H. H., Stahl, G. L., & Epand, R. M. (1987) *Proc. Natl. Acad. Sci. U.S.A. 84*, 7028–7030.

Susi, H., Sampugna, J., Hampson, J. W., & Ard, J. S. (1979) *Biochemistry 18*, 297–301.

Tamamura, H., Ikoma, R., Niwa, M., Funakoshi, S., Murakami, T., & Fujii, N. (1993a) *Chem. Pharm. Bull. 41*, 978–980.

Tamamura, H., Kuroda, M., Masuda, M., Otaka, A., Funakoshi, S., Nakashima, H., Yamamoto, N., Waki, M., Matsumoto, A., Lancelin, J. M., Kohda, D., Tate, S., Inagaki, F., & Fujii, N. (1993b) *Biochim. Biophys. Acta 1163*, 209–216.

Terwilliger, T. C., Weissman, L., & Eisenberg, D. (1982) *Biophys. J. 37*, 353–361.

Wald, J. H., Goormaghtigh, E., Meutter, J. D., Ruysschaert, J.-M., & Jonas, A. (1990) *J. Biol. Chem. 265*, 20044–20050.

Yonezawa, A., Kuwahara, J., Fujii, N., & Sugiura, Y. (1992) *Biochemistry 31*, 2998–3004.